

# A Hybrid $\Phi$ /B-OTDR for Simultaneous Vibration and Strain Measurement

Fei PENG\* and Xuli CAO

*Key Laboratory of Optical Fiber Sensing & Communications (Ministry of Education), University of Electronic Science and Technology of China, Chengdu, 611731, China*

\*Corresponding author: Fei PENG      E-mail: pengfei\_uestc@126.com

**Abstract:** A hybrid phase-sensitive optical time domain reflectometry ( $\Phi$ -OTDR) and Brillouin optical time domain reflectometry (B-OTDR) system which can realize simultaneous measurement of both dynamic vibration and static strain is proposed. Because the Rayleigh scattering light and spontaneous Brillouin scattering light are naturally frequency-multiplexed, the heterodyne asynchronous demodulation of frequency shift keying (FSK) in optical fiber communications is utilized, and the demodulations of the two scattering signals are synchronized. In addition, the forward Raman amplification is introduced to the system, which not only makes up for the deficiency of spontaneous Brillouin scattering based distributed fiber sensor, but also has the merit of the single end measurement of B-OTDR. The designed  $\Phi$ /B-OTDR hybrid system has the sensing range of 49 km with 10 m spatial resolution. The vibration and strain experiments show that this hybrid system has great potential for use in long-distance structural health monitoring.

**Keywords:** Optical fiber sensor; Rayleigh scattering; Brillouin scattering; vibration; strain

---

Citation: Fei PENG and Xuli CAO, "A Hybrid  $\Phi$ /B-OTDR for Simultaneous Vibration and Strain Measurement," *Photonic Sensors*, 2016, 6(2): 121–126.

---

## 1. Introduction

As the most attractive distributed fiber sensor (DFS), phase-sensitive optical time domain reflectometry ( $\Phi$ -OTDR) is successfully employed in the safety monitoring of petroleum, transportation, and structures where the vibration/sound waves need to be measured [1–5]. Especially in recent years, the distributed acoustic sensor, which is developed from  $\Phi$ -OTDR, is now being the most promising distributed fiber sensor [2]. To improve the sensing performance (including the sensitivity, sensing range, dynamic range, and bandwidth) of  $\Phi$ -OTDR, researchers focused on increasing the power of backscattered Rayleigh scattering (RS) light for

detecting the weak sensing signal RS with high signal noise ratio (SNR). No matter which kind of configuration being used, the nonlinear effects in the fiber have to be considered. The main nonlinear effect has been demonstrated to be modulation instability, which comes earlier than stimulated Brillouin scattering (BS) with the growing of the launching power of the probe pulse [3]. But BS still has to be considered even the stimulated BS does not occur, especially when the direct detection is employed (the spontaneous BS and RS are detected simultaneously) [4]. As to other aspect, in many applications, like structure health monitoring (SHM), after the vibration or acoustic wave generated by the structure transforming, the static strain (<0.1 Hz) of

---

Received: 30 August 2015 / Revised: 28 November 2015

© The Author(s) 2016. This article is published with open access at Springerlink.com

DOI: 10.1007/s13320-016-0289-9

Article type: Regular

the structure usually changes accordingly. But it is difficult to cover the ultra-low frequency for the current  $\Phi$ -OTDR or distributed acoustic sensor (DAS) [2]. In this article, by detecting spontaneous BS in  $\Phi$ -OTDR, a hybrid  $\Phi$ /B-OTDR (Brillouin optical time domain reflectometry) is proposed to simultaneously measure vibration (dynamic) and strain (static) in one sensing system. Therefore, a comprehensive analysis of vibration and strain can be realized by this hybrid system, offering more useful information for accurate estimation of structure health.

## 2. Principle of $\Phi$ /B-OTDR hybrid system

### 2.1 Wavelength relationship between the hybrid system and demodulator

Generally, the probe pulse of  $\Phi$ -OTDR is modulated by the acoustic optical modulator (AOM) for high extinction ratio pulse light. In this configuration, the wavelength relationship of laser, probe pulse, RS, and BS can be shown as Fig. 1.

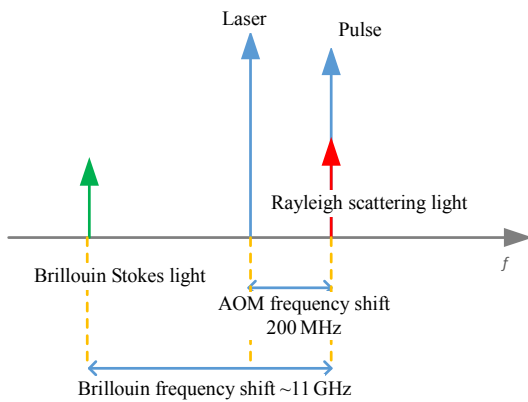


Fig. 1 Wavelength relationship of laser, probe pulse, RS, and BS in the hybrid system.

The frequency of pulse is upshifted by the AOM for 200 MHz (assuming the frequency shift of the AOM is 200 MHz). RS has the same frequency as the pulse and BS frequency downshift ( $\sim 11$  GHz). Utilizing the large frequency deviation of RS and BS and referring the principle of heterodyne asynchronous demodulation for frequency shift keying (FSK), we design the demodulator of the hybrid system, just as shown in Fig. 2. RS and BS

first beat with the local oscillator light, and then the mixed light is detected by a wide bandwidth detector ( $>11$  GHz). The radio frequency (RF) signal is divided by two branches. The upper branch demodulates the RS signal, and the lower branch demodulates the BS signal. The difference between this configuration and common heterodyne asynchronous demodulator for FSK is that the lower branch has to sweep the central frequency of the band pass filter (BPF) by a tunable BPF to fit the Brillouin spectrum of the fiber. After BPF, the envelopes of the mixed signals can be acquired by the envelope detectors. At last, the RS and BS curves can be sampled by the analog to digital (A/D) converter when the noise is further filtered by two low pass filters (LPFs).

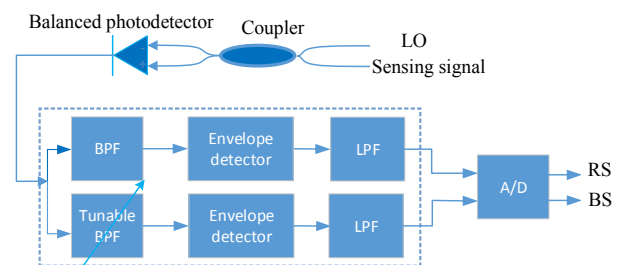


Fig. 2 Signal demodulation principle of the  $\Phi$ /B-OTDR system.

### 2.2 Synchronization principle in the demodulation

To realize the simultaneous demodulation of RS and BS signals, we design the demodulating synchronization mechanism, just as shown in Fig. 3. Instead of the polarization scrambling method, the polarization diversity method is used to ensure the RS signal to keep the polarization state of probe pulse stable in a relatively long time [6, 7]. After  $N \cdot T$  ( $T$  is the period of the light pulse, and  $N$  is the number of the light), the polarization of the local oscillator (LO) light is switched to polarization orthogonally to eliminate the polarization related gain of BS light by averaging the BS signal of the two LO polarizations. And the central frequency of the tunable BPF is changed around 11 GHz during each pulse repetition period to get the Brillouin

spectrum of each position. The RS is processed within  $N \cdot T$  (with the same LO polarization state during  $N \cdot T$ ) to avoid the polarization-induced intensity fluctuation of RS.

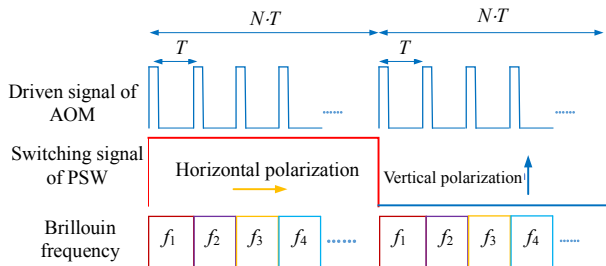


Fig. 3 Synchronization mechanism of the sensing signal demodulation.

### 3. Experiment

#### 3.1 Experimental setup

The schematic diagram of the hybrid system is shown in Fig. 4. A narrow line width ( $\sim 3$  kHz) semiconductor laser at 1550 nm is used. The laser is divided into two portions by 50:50 Coupler 1. One portion is modulated to pulse with the 2 kHz repetition rate and 100 ns pulse width. 200 MHz frequency shift is induced by using an AOM. Then the pulse light is amplified by an erbium doped fiber amplifier (EDFA) and passes to the BPF to suppress the amplified spontaneous emission noise generated by the EDFA. Then the pulse light launches into the fiber via a circulator. A Raman fiber laser with the central wavelength of 1455 nm is used as the Raman pump. The probe pulses are distributionally amplified by forward Raman pumps, generating RS light and spontaneous BS light along the fiber. Another portion of light split by Coupler 1 is used as a local oscillator with a polarization switch (PSW), which is used to eliminate the polarization related gain of BS. The local oscillator light is mixed with the RS signal by Coupler 2. Then, the beat light is detected by a balanced photodetector with the 11 GHz bandwidth and analyzed by an electronic spectrum analyzer (ESA). The BS and RS curves are sampled by an A/D card with 50 MSample/s. Finally, the sampled signal is processed by a computer in

real time. Using the demodulation method in Section 2, the vibration and strain information of the sensing fiber is updated with different speeds.

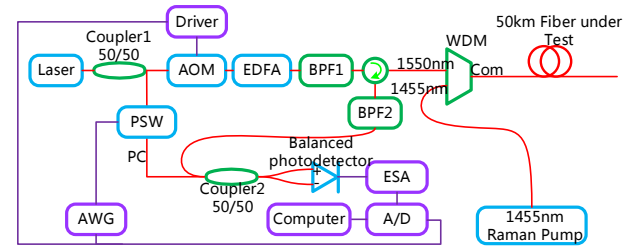


Fig. 4 Setup of the hybrid sensing system.

#### 3.2 Vibration test

When the probe pulse and RS light are enhanced by the former Raman pump, the RS curve obtained is shown in Fig. 5. It can be found that the power of the RS signal over the whole 49 km keeps relatively even by optimizing the power of pulse light and forward Raman pump [4], and the power difference of the fitting curve between the strongest and the weakest positions is less than 3 dB.

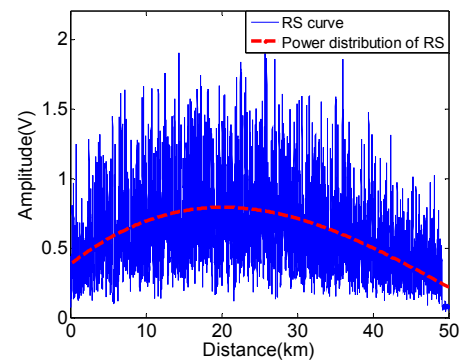


Fig. 5 RS curve acquired by the hybrid system.

To verify the vibration performance of this hybrid system, vibration measurement at the end of fiber is employed. We first spiral two-meter fiber at the distance of 49.03 km into a circle with the diameter of 10 cm and then paste it on the aluminum plate. The subtracted result of the adjacent two RS curves (16 times averaging) can be seen in Fig. 6. The maximum value of the subtracted curve appears at the distance of 49.03 km, where the ball drops.

We drop a ball at the location 49.03 km two times per second and storage the RS signals within

one second. And then the vibration level of each position is calculated by root-mean-square of each position, just as shown in Fig. 7. It can be found that the SNR of the vibration location is very high.

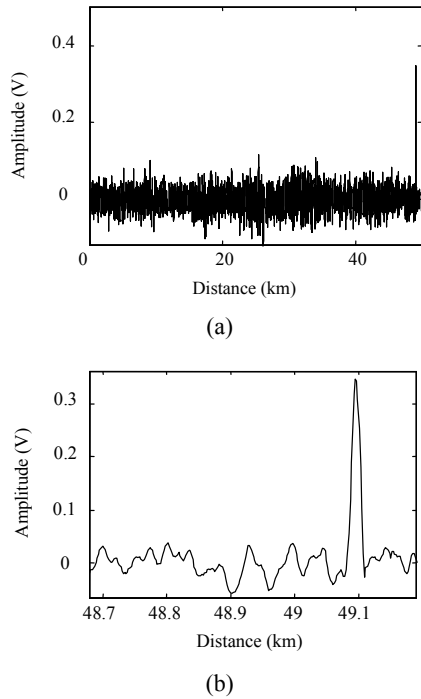


Fig. 6 Difference curve of RS of the falling ball (a) of all over the fiber and (b) near the vibration position when the falling ball experiment is employed.

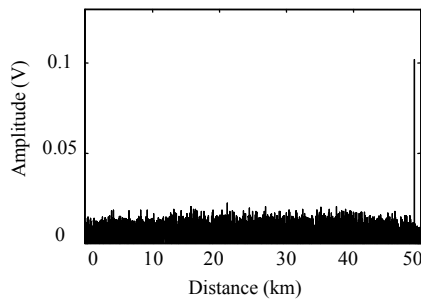


Fig. 7 Spatial distribution of vibration level when the falling ball experiment is employed.

### 3.3 Strain test

To verify the ability of measuring the static strain of the hybrid system, the strain experiment at the same position of vibration test, 49.03 km, is employed. The 10-m fiber is fixed on the micro-positioner. Then we adjust the strain imposed on the fiber from  $200\ \mu\epsilon$  to  $700\ \mu\epsilon$ . When the strain

is  $700\ \mu\epsilon$ , the spatial distribution of the BS spectrum can be seen as shown in Fig. 8(a). Compared with the configuration without forward Raman amplification, the power of the BS spectrum of the whole fiber is relatively flat, ensuring the strain to be accurate at the end of fiber.

The BS spectra near the strain point are shown in Figs. 8(b) and 8(c). We can see the obvious frequency shift of the BS spectrum near the strain point, and the BS spectrum of all locations has no obvious broadening.

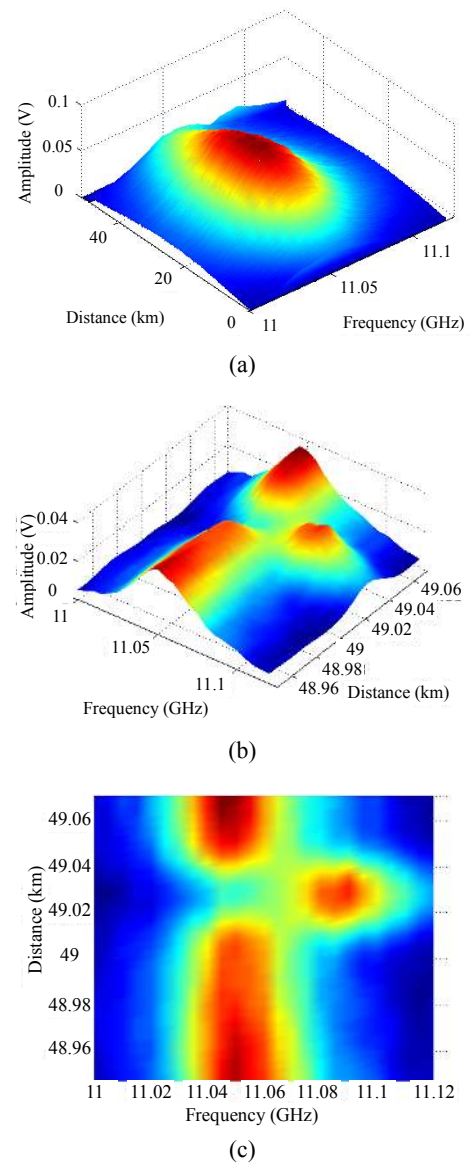


Fig. 8 BS spectra (a) of all over the fiber, (b) near the strain point, and (c) its vertical view.

By fitting the BS spectra of all positions, we can get Brillouin frequency shift (BFS) of each location, as shown in Fig. 9.

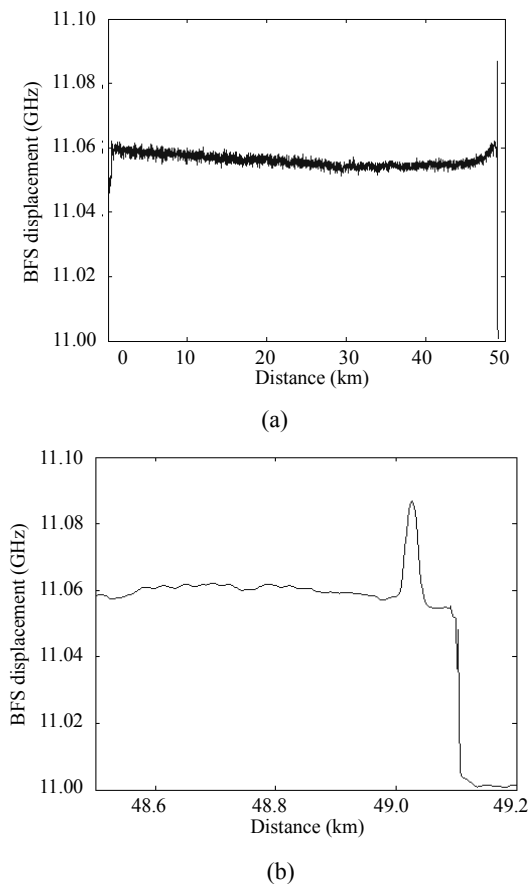


Fig. 9 BFS distributions (a) of all over the fiber and (b) near the strain point when the strain is  $700\mu\epsilon$ .

The spatial distribution of BFS under different strains can be seen in Fig. 10.

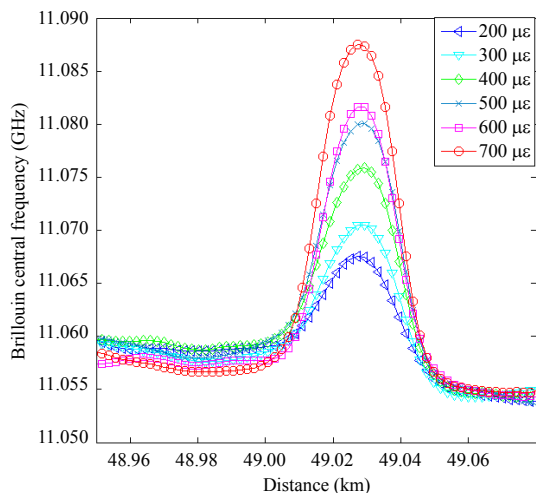


Fig. 10 Spatial distribution of BFS under different strains.

Because the strain experiment is not in constant temperature environment, we calibrate the peak value of Brillouin frequency shift under each strain by subtracting the peak value of Brillouin frequency shift at the location where fiber has natural conditions. Finally, we get the relationship between the strain and BFS of the strain point, as shown in Fig. 11. The strain and BFS have good linearity, and the norm of residual standard error is 1.2911 MHz.

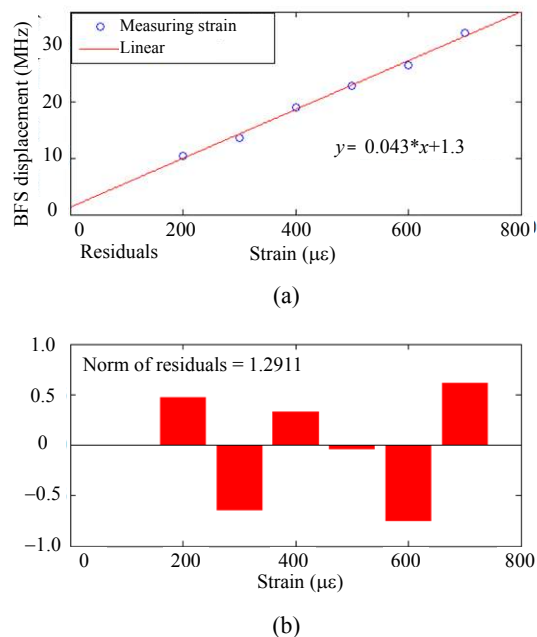


Fig. 11 Relationship between the strain and BFS displacement (a) and the residual of strain (b) when different strains are imposed.

### 4. Conclusions

In this article, a hybrid  $\Phi$ /B-OTDR for simultaneous vibration and strain is proposed. Utilizing the heterodyne detection configuration of classical FSK communications, RS and BS signals in the fiber can be simultaneously detected by the designed synchronization mechanism. To keep the advantage of single-end measurement, we introduce the forward Raman amplification to the system. Not only the sensing range is extended, but also the measurement deficiency of the spontaneous-Brillouin-based DFS (distributed fiber sensor) compared with stimulated-Brillouin-based DFS is also made up for. To verify the sensing

performance of the system, the vibration and strain at 49 km are measured successfully with 10 m spatial resolution.

This system has the advantages of long distance, single-end, and dual-parameter measurement, making it possible to be applied in long-distance SHM in future.

### Acknowledgment

This work is supported by the National Nature Science Foundation of China (NSFC) under grants (61290312 and 61205048), the PCSIRT (IRT1218), and the 111 Project (B14039).

**Open Access** This article is distributed under the terms of the Creative Commons Attribution 4.0 International License (<http://creativecommons.org/licenses/by/4.0/>), which permits unrestricted use, distribution, and reproduction in any medium, provided you give appropriate credit to the original author(s) and the source, provide a link to the Creative Commons license, and indicate if changes were made.

### References

- [1] J. C. Juarez and H. F. Taylor, "Field test of a distributed fiber-optic intrusion sensor system for long perimeters," *Applied Optics*, 2007, 46(46): 1968–1971.
- [2] T. R. Parker, A. Gillies, S. V. Shatalin, and M. Farhadiroushan, "The intelligent distributed acoustic sensing," in *Proc. SPIE*, vol. 9157, pp. 91573Q-1–91573Q-4, 2014.
- [3] H. F. Martins, S. Martin-Lopez, P. Corredera, P. Salgado, O. Frazão, and M. González-Herráez, "Modulation instability-induced fading in phase-sensitive optical time-domain reflectometry," *Optics Letters*, 2013, 38(6): 872–874.
- [4] F. Peng, H. Wu, X. H. Jia, Y. J. Rao, Z. N. Wang, and Z. P. Peng, "Ultra-long high-sensitivity  $\Phi$ -OTDR for high spatial resolution intrusion detection of pipelines," *Optics Express*, 2014, 22(11): 13804–13810.
- [5] F. Peng, N. Duan, Y. Rao, and J. Li, "Real-time position and speed monitoring of trains using phase-sensitive OTDR," *IEEE Photonic Technology Letters*, 2014, 26(20): 2055–2057.
- [6] X. Zhang, Y. Lu, F. Wang, H. Liang, and Y. Zhang, "Development of fully-distributed fiber sensors based on Brillouin scattering," *Photonic Sensors*, 2011, 1(1): 54–61.
- [7] T. Horiguchi, K. Shimizu, T. Kuroshima, M. Tateda, and Y. Koyamada, "Development of a distributed sensing technique using Brillouin scattering," *Journal of Lightwave Technology*, 1995, 13(7): 1296–1302.